

## Accurate first-order transition points from finite-size data without power-law corrections

W. Janke

*Institut für Theoretische Physik, Freie Universität Berlin, Arnimallee 14, 1000 Berlin 33, Germany  
and Höchstleistungsrechenzentrum, Forschungszentrum Jülich, Postfach 1913, 5170 Jülich, Germany*

(Received 5 October 1992)

Traditional observables used to locate first-order phase-transition points from Monte Carlo simulations on finite lattices usually exhibit powerlike finite-size scaling behavior. For systems in a box of volume  $V$  with periodic boundary conditions, several definitions of finite volume (pseudo-) transition temperatures  $T_0(V)$  have recently been proposed which involve only exponential corrections with respect to  $T_0 \equiv T_0(\infty)$ . One of these approaches suggests also a different and efficient way to compute the latent heat. These propositions are tested for the temperature-driven first-order phase transitions in the two-dimensional  $q$ -state Potts model for  $q=5, 8$ , and  $10$  by means of Monte Carlo simulations, using the single-cluster update algorithm and histogram reweighting techniques.

### I. INTRODUCTION

In the idealized infinite-volume limit, first-order phase transitions are characterized by discontinuities in the first derivative of the free energy. For a temperature- or field-driven transition this gives rise to jumps in the internal energy or the magnetization, and consequently to  $\delta$ -function singularities of the specific heat or the susceptibility. In a finite volume  $V$  these singularities are smoothed out and, depending on its strength, the transition is signaled by more or less pronounced finite peaks of the specific heat or susceptibility near the infinite-volume transition point.

If the volume is cubic or nearly cubic, the width of the peak is proportional to  $1/V$ , and the location of the peak maximum is shifted by an amount  $O(V^{-\alpha})$  with respect to the actual infinite-volume transition temperature  $T_0$ , where  $\alpha > 0$  depends on the model and the type of boundary conditions.<sup>1-6</sup> Typically one has  $\alpha=1$  and may try to estimate  $T_0 \equiv 1/\beta_0$  from the peak locations on finite lattices by extrapolations in  $1/V$ .

Related definitions of finite-volume transition points are based on various ratios of moments of the energy or magnetization distribution. The most popular is the so-called Binder parameter<sup>7</sup> (here and in the following we shall illustrate the concepts only for temperature-driven transitions):

$$B(V, \beta) = 1 - \frac{\langle E^4 \rangle}{3\langle E^2 \rangle^2}, \quad (1)$$

where  $\langle \cdot \rangle$  denotes thermal averages in a finite volume  $V$  and  $E$  is the energy of the system. In the idealized infinite-volume limit,  $B$  has an isolated minimum  $B(T_0) < \frac{2}{3}$  at the transition point  $T_0$ , while  $B = \frac{2}{3}$  away from the transition. In a finite volume this discontinuity is again smoothed out and the location of the minimum is shifted by an amount proportional to  $V^{-\alpha}$  if the volume is approximately cubic.<sup>8</sup> For the most common situations one finds again  $\alpha=1$ .<sup>9</sup>

Another useful observable is the low-order variant of

(1) with  $E^4$  replaced by  $E^2$  and  $E^2$  by  $E$ . These observables are sensitive to the (additive) energy normalization of the model. Such a dependence is avoided in the connected Binder parameter

$$B^c(V, \beta) = 1 - \frac{\langle (E - \langle E \rangle)^4 \rangle}{3\langle (E - \langle E \rangle)^2 \rangle^2}, \quad (2)$$

which is closely related to the second derivative of the specific heat. In a finite volume it has a smooth peak in the vicinity of the transition point. The location of the maximum is again displaced from  $T_0$  by an amount proportional to  $V^{-\alpha}$  with typically  $\alpha=1$ . A simple rigorous bound is  $B^c(V, \beta) \leq \frac{2}{3}$ .

In Monte Carlo simulation studies, due to unavoidable statistical errors, extrapolations of finite-volume data are not always reliable. Apart from these (hopefully) random and uncorrelated statistical errors the data are also systematically shifted by additional exponential corrections which are difficult to take into account theoretically. But a precise knowledge of the infinite-volume limit is often important since many quantities of physical interest are just defined at the (*a priori* unknown) transition point  $T_0$ . It is therefore desirable to find definitions of a finite-volume transition point which involve *no* power-law corrections at all. Such definitions will be provided by the new observables introduced in Sec. II. The practical applicability of these propositions is tested numerically for the temperature-driven first-order phase transition of the two-dimensional  $q$ -state Potts model with  $q=5, 8$ , and  $10$ . In Sec. III, the setup of the Monte Carlo simulations using the single-cluster update algorithm and the methods of data analyses are described, and in Sec. IV, the results are presented. Finally, Sec. V contains the conclusions.

### II. THE NEW OBSERVABLES

Let us start with one possible definition that has already been given in Refs. 10 and 11 (see also Ref. 12). The derivation is based on the observation that on lattices with periodic boundary conditions, the partition

function of a model describing the coexistence of one disordered and  $q$  ordered phases can be written for large enough  $q$  as<sup>13</sup>

$$Z_{\text{per}}(V, \beta) = \left[ \sum_{m=0}^q e^{-\beta f_m(\beta)V} \right] [1 + O(Ve^{-L/L_0})]. \quad (3)$$

Here  $L_0 < \infty$  is a constant,  $L$  is the linear length of the lattice,  $\beta \equiv 1/k_B T$  is the inverse temperature, and  $f_m(\beta)$  is the metastable free-energy density of the phase  $m$ . It can be defined in such a way that it is equal to the idealized infinite-volume free-energy density  $f(\beta)$  if  $m$  is stable and strictly larger than  $f(\beta)$  if  $m$  is unstable.<sup>10,11</sup> This implies that the parameter

$$N(\beta) = \lim_{V \rightarrow \infty} Z_{\text{per}}(V, \beta) e^{\beta f(\beta)V} \quad (4)$$

is equal to the number of stable phases at the inverse temperature  $\beta$ . With increasing temperature  $N(\beta)$  thus takes the values  $q$ ,  $q+1$ , and 1. Since  $N(\beta)$  has an isolated maximum at the transition point where the  $q+1$  phases coexist, a natural definition of a finite-volume transition point  $\beta_0(V)$  is the point where a suitable finite-size approximation to  $N(\beta)$ , say

$$N(V, \beta) = Z_{\text{per}}(V, \beta) e^{\beta f(\beta)V}, \quad (5)$$

is maximal. The important observation is that, due to the bound (3) (and similar bounds for derivatives<sup>10,11</sup>), this definition leads only to exponentially small shifts of  $\beta_0(V)$  with respect to the infinite-volume transition point  $\beta_0$ .

For an actual numerical determination of  $\beta_0(V)$  the criterion (5) is not yet well suited. While the partition function  $Z_{\text{per}}(V, \beta)$  can actually be measured in Monte Carlo simulations (except for an irrelevant  $\beta$ -independent constant), the free energy  $f(\beta)$  is only defined in the thermodynamic limit and hence not accessible to numerical simulations. It is therefore necessary to eliminate this term by, e.g., forming a suitable ratio. Instead of (5) one may look for the maximum of the *number-of-phases* parameter

$$N(V_1, V_2, \beta) = \left[ \frac{Z_{\text{per}}(V_1, \beta)^\alpha}{Z_{\text{per}}(V_2, \beta)} \right]^{1/(\alpha-1)}, \quad (6)$$

where  $\alpha = V_2/V_1$ .<sup>12</sup> By inserting (3) it is straightforward to verify that  $N(V_1, V_2, \beta)$  behaves qualitatively as  $N(\beta)$ . With increasing temperature it smoothly interpolates between the values  $q$ ,  $q+1$ , and 1. The value of  $\beta$  at the maximum is then the desired, only exponentially shifted finite-volume transition point  $\beta_0(V)$  which will be denot-

ed  $\beta_{V/V}$ . Differentiating  $\ln N$  with respect to  $\beta$  we see that determining  $\beta_{V/V}$  amounts to solving  $\alpha E(V_1, \beta_{V/V}) = E(V_2, \beta_{V/V})$  or  $e(V_1, \beta_{V/V}) = e(V_2, \beta_{V/V})$ , i.e., to locating the crossing point of the internal energies per site,  $e \equiv E/V$ , on the two lattices of different size.

Obviously the numerical determination of  $\beta_{V/V}$  requires simulations on two different lattices. In Ref. 12, we have therefore proposed another definition of a finite-size transition point which requires data from one lattice only. Its definition is based on the fact that the partition function of a statistical system may be written as<sup>14</sup>

$$Z = \sum_{\text{configurations}} e^{-\beta E} = \sum_E N(E) e^{-\beta E}, \quad (7)$$

where  $N(E)$  is the number of configurations with the energy  $E$ . In practice, by recording energy histograms, one measures the closely related probability distribution

$$P_\beta(E) = \frac{1}{Z} N(E) e^{-\beta E}, \quad (8)$$

which, in the vicinity of a first-order transition point, has the typical double-peak form depicted for three characteristic temperatures in Fig. 1. The different shapes are related to each other via the relation

$$P_{\beta'}(E) \propto P_\beta(E) e^{-(\beta' - \beta)E}. \quad (9)$$

This is the basis for the recently popularized<sup>15,16</sup> so-called reweighting technique which is quite essential for the technical feasibility of the method of Ref. 12 to be described next.

At the infinite-volume transition point all free energies  $f_m(\beta)$  are equal, so that Eq. (3) implies

$$w_o \equiv \sum_{m=1}^q e^{-\beta_0 f_m(\beta_0)V} = q e^{-\beta_0 f_d(\beta_0)V} \equiv q w_d, \quad (10)$$

apart from exponentially small corrections. Here the free-energy density of the "zeroth," disordered phase is denoted by  $f_d$ , and  $w_{o,d}$  are the associated statistical weights of the coexisting phases. A natural definition of a finite-volume transition point  $\beta_w$  is thus the point where the ratio of the total weight of the  $q$  ordered phases to the weight of the disordered phase approaches  $q$ . More precisely we introduce the *ratio-of-weights* parameter

$$R(V, \beta) \equiv \frac{\sum_{E < E_0} P_\beta(E)}{\sum_{E \geq E_0} P_\beta(E)}, \quad (11)$$

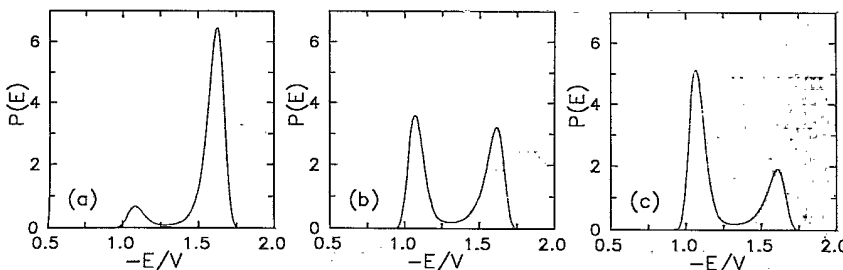


FIG. 1. The typical double-peak form of the probability distribution  $P_\beta(E)$  on finite lattices in the vicinity of a first-order transition for three characteristic temperatures: (a)  $\beta_0$ , the infinite volume transition point, (b)  $\beta_{C_{\text{max}}}$ , the position of the specific-heat maximum, and (c)  $\beta_{B_{\text{min}}}$ , the position of the Binder-parameter minimum. The data are actual simulation results for  $q=8$  and  $V=57 \times 57$ .

and determine  $\beta_W$  by solving

$$R(V, \beta_W) = q. \quad (12)$$

For notational convenience we shall often write  $R = W_o/W_d$  with  $W_{o,d}(V, \beta)$  identified with the numerator and denominator in (11), respectively. The parameter  $E_0$  in (11) is defined by reweighting the energy distribution to the temperature where both peaks of  $P_\beta(E)$  have equal height and then taking  $E_0$  as the energy at the minimum between the two peaks. Clearly, also other definitions of  $E_0$  would be reasonable as well, as, for example, the internal energy at the temperature where the specific heat is maximal. Since it is expected that the relative height of the minimum between the two peaks decreases like  $e^{-\text{const}L^{d-1}}$  as  $L \rightarrow \infty$ , all these definitions do, in fact, only differ by exponentially small errors. It is therefore a matter of practical convenience to choose  $E_0$ . Obviously, in order to solve Eq. (12), the reweighting technique is an optimal tool.

Note that in (12) we have assumed that the number of ordered phases,  $q$ , is known by general arguments. If this is not the case, one may use the crossing points  $\beta_{W/W}$  satisfying

$$R(V_1, \beta_{W/W}) = R(V_2, \beta_{W/W}) \quad (13)$$

as estimates for  $\beta_0$ . The value of  $R$  at the crossing point then gives the ratio of the number of coexisting ordered and disordered phases. This, of course, requires again the simulation on two different lattices.

Clearly, all these considerations apply to field-driven first-order transitions as well. The point  $\beta_{V/V}$ , e.g., should then be replaced by the position  $h_{V/V}$  of the maximum of ratio (6) as a function of field  $h$ . And instead of energy histograms one should use magnetization histograms.

### III. THE SIMULATION

We have tested the propositions of Sec. II by Monte Carlo simulations of the two-dimensional  $q$ -state Potts model<sup>17</sup> on square lattices with  $q = 5, 8$ , and 10. The energy of the Potts model is given by

$$E = - \sum_{\langle \mathbf{x}, \mathbf{x}' \rangle} \delta_{s(\mathbf{x})s(\mathbf{x}')}, \quad (14)$$

where the spins  $s(\mathbf{x})$  at each lattice site  $\mathbf{x}$  take the integer values  $1, \dots, q$ ,  $\delta_{ss'}$  is Kronecker's symbol, and the sum-

mation runs over all nearest-neighbor pairs. We always employ the periodic boundary condition. The two-dimensional Potts model is a convenient toy model for testing new ideas since for  $q \geq 5$  it is *exactly* known<sup>17,18</sup> to exhibit a temperature-driven first-order phase transition at  $\beta_0 = \ln(1 + \sqrt{q})$ . Furthermore, right at the transition also the internal energies of the disordered and ordered phases,  $\hat{e}_d, \hat{e}_o$ , and the difference of the corresponding specific heats,  $\Delta\hat{c} \equiv \hat{c}_d - \hat{c}_o$ , are known exactly.<sup>17,18</sup> A brief summary is given in Appendix A. A glance on the transition entropies,  $\Delta\hat{s}$ , compiled in Table I shows that our choice of  $q$  values covers the whole range from very weak to rather strong first-order phase transitions.

To update the spin configurations we have used the cluster algorithm<sup>19</sup> in its single-cluster variant<sup>20</sup> which is very successful in reducing critical slowing down near continuous phase transitions. At the first-order transitions considered here, however, the overall gain in CPU time as compared to the standard Metropolis algorithm turned out to be only quite modest. As a general rule the efficiency decreases with increasing  $q$ , i.e., with increasing strength of the first-order transition. And it appeared to be more efficient to perform the simulations on the high-temperature side of the transition. More details of these dynamical aspects of the single-cluster update will be reported in a separate publication.<sup>21</sup>

For each  $q$  and lattice size, we have first performed one relatively short simulation at the exactly known transition point  $\hat{\beta} = \beta_0 = \ln(1 + \sqrt{q})$  and recorded the (normalized) energy histogram  $P_{\hat{\beta}}(E)$ . Using relation (9) this allows one, in principle, to calculate the energy distribution and hence expectation values at any inverse temperature  $\beta$ .<sup>15</sup> In Monte Carlo studies of first-order phase transitions the actual range of  $\beta$  is limited by statistical errors to  $|\beta - \hat{\beta}|E = O(1)$ , i.e.,  $|\beta - \hat{\beta}| = O(1/V)$ , but this is still wide enough to get estimates  $\beta_1$  and  $\beta_2$  of the specific-heat maximum and the Binder-parameter minimum, respectively. We have then performed three rather long simulations at  $\beta_0, \beta_1$ , and  $\beta_2$ , and recorded again the energy histograms. Their typical shapes can be inspected in Fig. 1. In general, for nontrivial models with unknown  $\beta_0$ , one would run the short simulation at some  $\hat{\beta}$  near the transition point and use Eq. (12) to get a first rough estimate of  $\beta_0$ . Finally, basically applying again Eq. (9), we have combined the three histograms at fixed  $q$  and  $V$  to a single, optimized histogram,<sup>16</sup> which was then used for all further analyses. As a typical example Fig. 2 shows the relative weights for the optimal combination of the

TABLE I. Exact results for the two-dimensional  $q$ -state Potts model.

	$q=5$	$q=8$	$q=10$
$\beta_0 = \ln(1 + \sqrt{q})$	1.174 359	1.342 454	1.426 062
$T_0 = 1/\beta_0$	0.851 528	0.744 904	0.701 232
$(\hat{e}_d + \hat{e}_o)/2 = 1 + 1/\sqrt{q}$	1.447 214	1.353 554	1.316 228
$\Delta\hat{e} = \hat{e}_d - \hat{e}_o$ [see Eq. (A3)]	0.052 919	0.486 358	0.696 050
$-\hat{e}_d$	1.420 754	1.110 374	0.968 203
$-\hat{e}_o$	1.473 673	1.596 733	1.664 253
$\Delta\hat{s} = \beta_0 \Delta\hat{e}$	0.062 146	0.652 914	0.992 610
$\Delta\hat{c} = \beta_0 \Delta\hat{s} / \sqrt{q}$	0.032 638	0.309 892	0.447 628

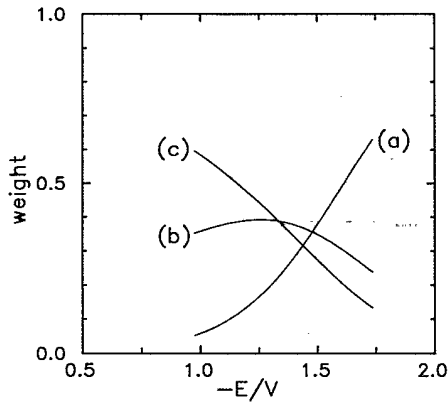


FIG. 2. The weights determined in the computation of the optimized histogram from the three histograms shown in Fig. 1.

three histograms in Fig. 1. As is clear from Fig. 1, our choice of simulation points is a well-defined educated guess, giving a quite uniform accuracy for the optimized histogram. It is, however, clearly not crucial at this point to determine  $\beta_{C_{\max}}$  and  $\beta_{B_{\min}}$ , the true location of the extrema of the specific heat and Binder parameter, or the usually unknown<sup>22</sup> transition point  $\beta_0$  with high precision.

Depending on  $q$  (and thus the strength of the transi-

TABLE II. Simulation points  $\beta_1$  ( $\approx$  specific-heat maximum) and  $\beta_2$  ( $\approx$  Binder-parameter minimum) as determined from a short test run. A third long simulation was performed at the exactly known infinite-volume transition point  $\beta_0 = \ln(1 + \sqrt{q})$ . The statistics is given in units comparable to Metropolis sweeps,  $t_{\text{run}} = (\langle |C| \rangle / V) \times \text{number of simulated clusters}$ , with  $\langle |C| \rangle$  denoting the average cluster size.

$L$	$q=5$		$\beta_0$	$t_{\text{run}}/10^6$	
	Simulations at $\beta_1$	$\beta_2$		$\beta_1$	$\beta_2$
20	1.163 1	1.157 36	2.17	2.24	2.23
26	1.163 79	1.159 138	2.03	1.67	1.52
34	1.169 27	1.167	1.91	1.93	2.00
44	1.170 908 1	1.169 677	1.81	1.81	1.95
57	1.172	1.170 96	2.13	2.01	2.17
74	1.172 88	1.172 47	2.54	2.81	2.90
	$q=8$				
15	1.328 362	1.322 8	1.96	1.99	1.74
20	1.333 275	1.332	1.89	1.77	1.91
26	1.336 61	1.334	1.86	1.71	1.07
34	1.339 05	1.337 61	2.55	2.37	1.80
44	1.340 4	1.339 5	2.70	2.54	1.78
57	1.341 29	1.340 84	2.81	3.12	2.91
	$q=10$				
12	1.406 27	1.395	4.31	2.51	1.41
15	1.413 05	1.408 5	2.09	1.63	1.65
20	1.418	1.414 5	2.75	2.08	1.59
26	1.421 39	1.419 4	1.36	1.40	1.27
34	1.423 207	1.421 87	3.89	3.39	2.32

tion) and  $V$ , the run time  $t_{\text{run}}$  of the long simulations was of order  $(1.1-4.3) \times 10^6$ . Here  $t_{\text{run}}$  is defined in units comparable to Metropolis sweeps as  $(\langle |C| \rangle / V) \times N_c$ , where  $\langle |C| \rangle$  denotes the average cluster size and  $N_c$  is the number of simulated clusters. See Table II for more details concerning the statistics of the simulations. With our implementation of the single-cluster update on a CRAY X-MP 2/4 it takes, on the average, about 4  $\mu\text{sec}$  to update one spin. For comparison, our vectorized single-hit Metropolis code requires only around 0.7  $\mu\text{sec}$  on the same machine.

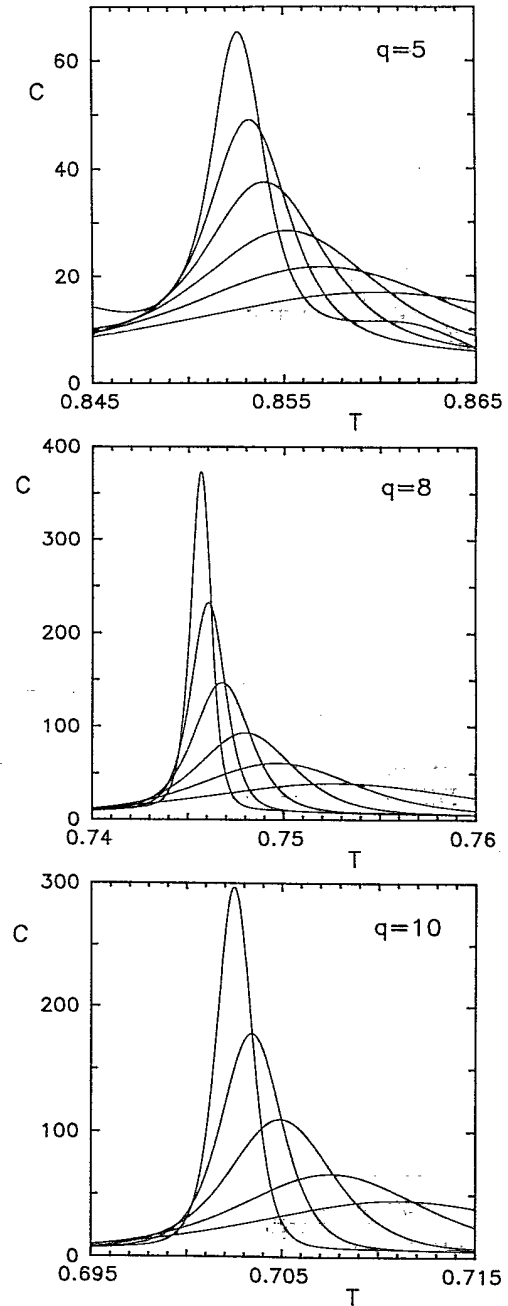


FIG. 3. The specific heat for  $q=5, 8,$  and  $10$  for various lattice sizes computed by reweighting the optimized histograms.

## IV. RESULTS

## A. Transition points from traditional observables

Let us start with analyses of the traditional observables which we shall need for comparison with the new approaches described in Sec. II. In Figs. 3 and 4 we plot for  $q=5, 8,$  and  $10$  the specific heat,  $C$ , and Binder parameter,  $B$ , curves versus temperature as obtained from the optimized histograms. The maxima of  $C$  and the minima of  $B$  define the pseudotransition temperatures  $T_{C_{\max}}$  and

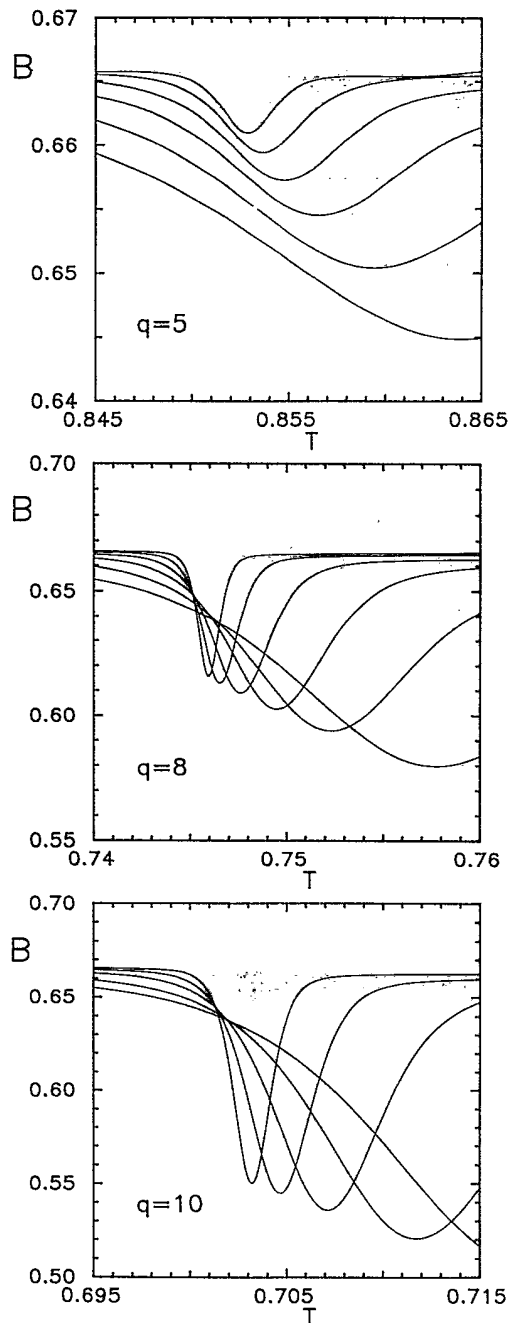


FIG. 4. The Binder parameter for  $q=5, 8,$  and  $10$  for various lattice sizes computed by reweighting the optimized histograms.

$T_{B_{\min}}$ . The finite-size scaling of the Binder parameter at  $T_0$ ,  $T_{C_{\max}}$ , and  $T_{B_{\min}}$  is depicted in Fig. 5. The arrows on the y axis show the exactly known infinite-volume limits (see Table III and Appendix B). In Fig. 6, we also show the related connected Binder parameter defined in Eq. (2). The blowups on the right-hand panels demonstrate that the curves for different lattice sizes cross each other quite nicely around  $T_0$  and thus may also be used for locating the transition point. The positions of the specific-heat maximum and Binder-parameter minimum for  $q=5, 8,$  and  $10$  are plotted versus  $1/V$  in Fig. 11 where they are compared with the results of the new criteria to locate  $\beta_0$ , to be discussed in the next subsection. The solid lines

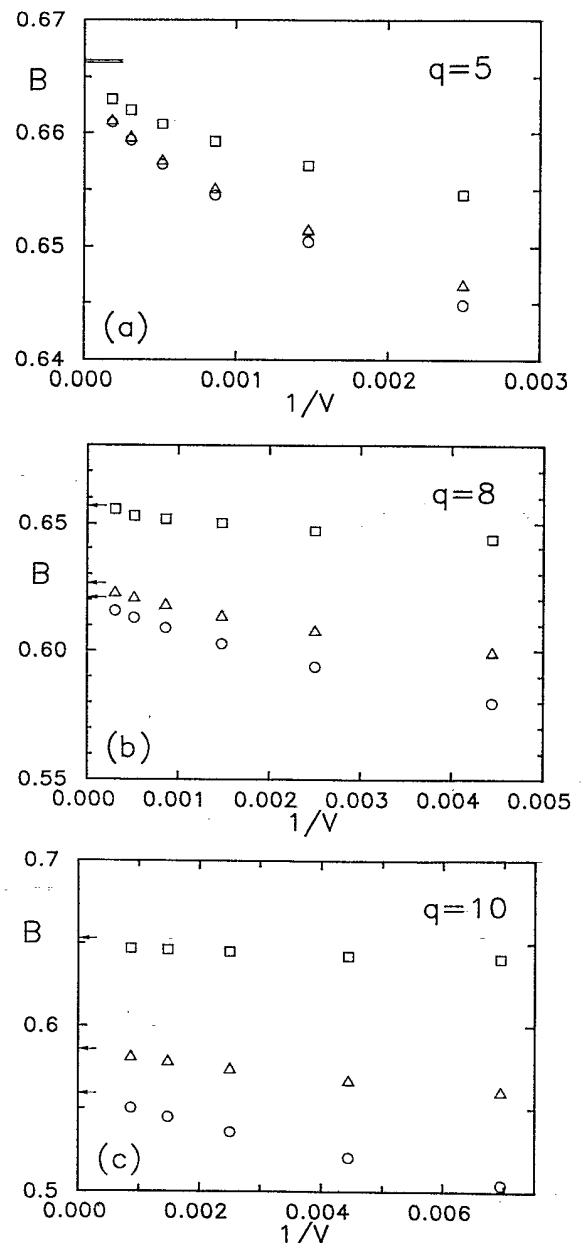


FIG. 5. Finite-size scaling of the Binder parameter at  $T_0$  ( $\square$ ),  $T_{C_{\max}}$  ( $\triangle$ ), and  $T_{B_{\min}}$  ( $\circ$ ). The arrows on the y axis show the exactly known infinite-volume limits.

TABLE III. Exactly known coefficients in the asymptotic finite-size scaling expansions for the two-dimensional  $q$ -state Potts model.

		$q=5$	$q=8$	$q=10$
$C(T_0)=AV+\dots$	$A$	0.000 536	0.042 103	0.081 428
$C(T_{B_{\min}})=AV+\dots$	$A$	0.000 964	0.936 613	0.186 143
$C_{\max}=AV+\dots$	$A$	0.000 966	0.106 574	0.246 319
$T_{C_{\max}}=T_0+a_1/V+a_2/V^2+\dots$	$a_1$	22.052 7	2.372 42	1.626 67
	$a_2$	233.982	3.749 34	2.001 47
$T_{B_{\max}}=T_0+a_1/V+a_2/V^2+\dots$	$a_1$	22.052 7	2.372 42	1.626 67
	$a_2$	884.331	9.080 17	4.206 40
$B(T_0)=a_0+\dots$	$a_0$	0.666 431	0.656 786	0.653 018
$B(T_{C_{\max}})=a_0+\dots$	$a_0$	0.666 221	0.626 279	0.585 234
$B_{\min}=a_0+\dots$	$a_0$	0.666 221	0.620 711	0.558 909
$T_{B_{\min}}=T_0+a_1/V+\dots$	$a_1$	23.054 928	3.201 306	2.392 021

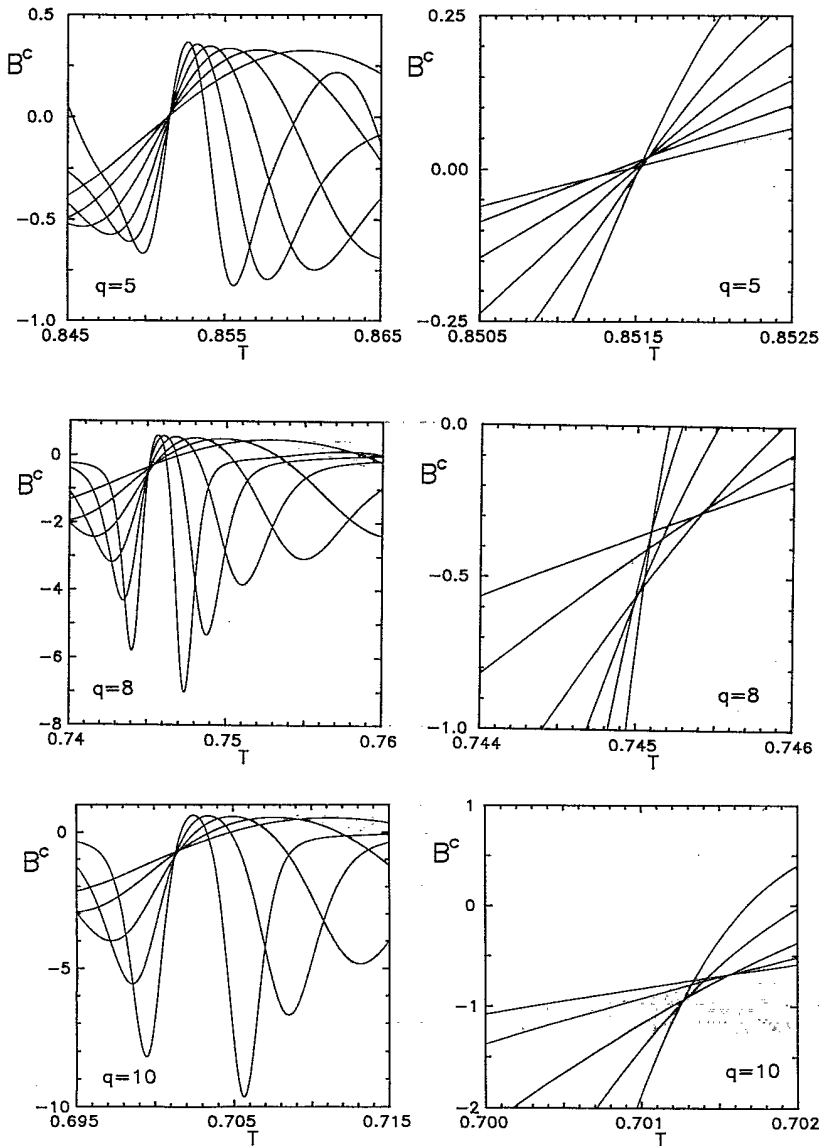


FIG. 6. The connected Binder parameter for  $q=5, 8$ , and  $10$  for various lattice sizes computed by reweighting the optimized histograms. The right-hand panels show a magnification of the crossing region.

show the infinite-volume transition points and the leading  $1/V$  corrections, which are also exactly known for the two-dimensional (2D) Potts model. Neglecting the exponential corrections and rewriting the basic formula (3) as

$$Z_{\text{per}} = 2\sqrt{q} e^{-V\beta(f_o+f_d)/2} \cosh \left[ V\beta \frac{f_d-f_o}{2} + \frac{1}{2} \ln q \right], \quad (15)$$

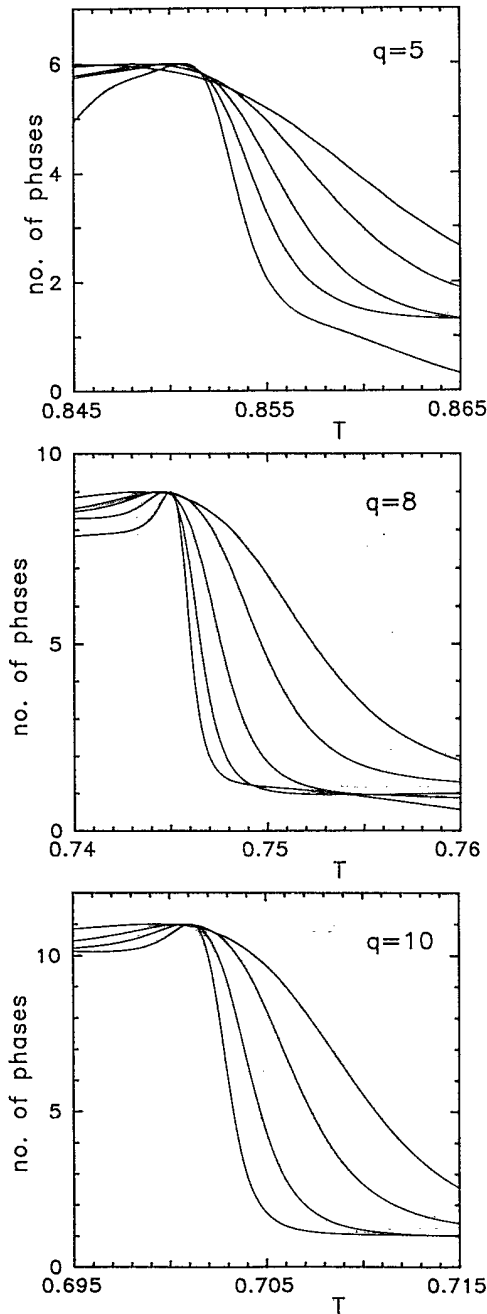


FIG. 7. The number-of-phases parameter in Eq. (6) for  $q=5, 8,$  and  $10$  for various lattice sizes computed by reweighting the optimized histograms. For each curve the maximum is normalized to  $q+1$ .

it is straightforward but tedious to derive the  $1/V$  expansions of cumulants by differentiation of  $\ln Z_{\text{per}}$  with respect to  $\beta$ . The results can be found in Ref. 23, albeit in a quite cumbersome notation. We have therefore repeated this calculation and expressed the expansion coefficients in more physical terms like the latent heat, etc. (see Appendix B). We have carefully checked that all formulas agree with the results in Ref. 23.

The leading terms may also be derived somewhat more heuristically from a simple two-phase model assuming that the system spends a fraction  $W_o$  of the total time in the ordered phases (with energy  $\hat{e}_o$ ) and a fraction  $W_d=1-W_o$  in the disordered phase (with energy  $\hat{e}_d$ ). Within this simple picture the tunneling events are approximated by sharp jumps and all fluctuations within the phases are neglected. Consequently,  $\langle e^n \rangle = W_o \hat{e}_o^n + (1-W_o) \hat{e}_d^n$ , and the specific heat,

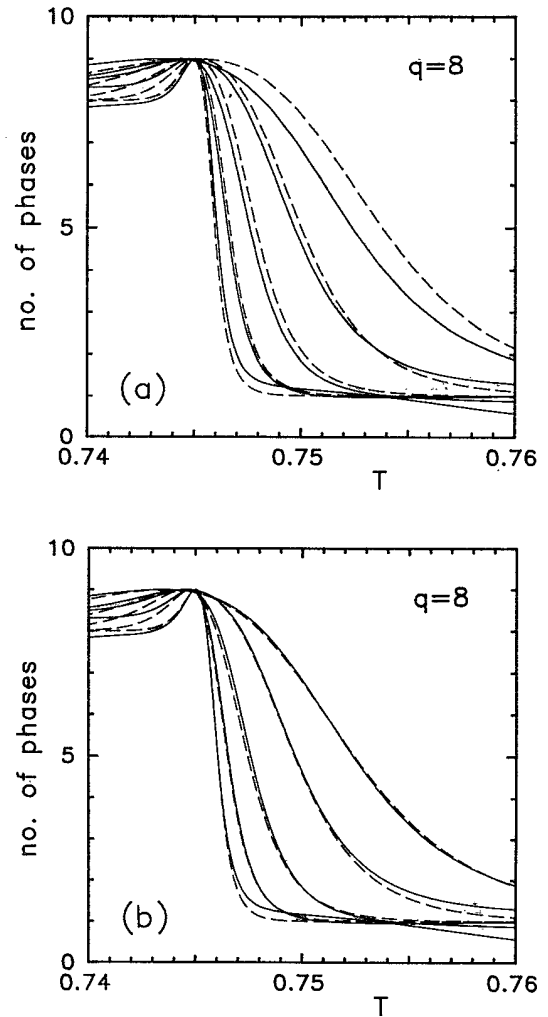


FIG. 8. Comparison of the finite-size scaling form (16) (---) for the number-of-phases parameter with the actual data for  $q=8$  (—) computed by reweighting the optimized histograms. In (a) the exactly known transition temperature  $T_0=1/\ln(1+\sqrt{q})$  is used, and in (b)  $T_0$  is replaced by the measured values  $T_{V/\gamma}$ .

$$C = V\beta^2(\langle e^2 \rangle - \langle e \rangle^2) = V\beta^2 W_o(1 - W_o)\Delta\hat{e}^2,$$

is easily seen to have a maximum,  $C_{\max} = V\beta_o^2(\Delta\hat{e}/2)^2$ , for  $W_o = W_d = \frac{1}{2}$ , i.e., for an energy distribution with two peaks of equal weight. Here we have defined  $\Delta\hat{e} \equiv \hat{e}_d - \hat{e}_o$ . The peak location  $\beta_{C_{\max}} = \beta_o - \ln q / V\Delta\hat{e} + \dots$  follows then from the expansion

$$\begin{aligned} \ln(W_o/W_d) &= \ln q + V\beta(f_d - f_o) \\ &= \ln q + V\Delta\hat{e}(\beta - \beta_o) + \dots \end{aligned}$$

Similarly, the minimum of the Binder parameter,  $B_{\min} = 1 - (\hat{e}_o/\hat{e}_d + \hat{e}_d/\hat{e}_o)^2/12$ , is found at a weight ratio  $W_o/W_d = \hat{e}_d^2/\hat{e}_o^2 < 1$ , implying

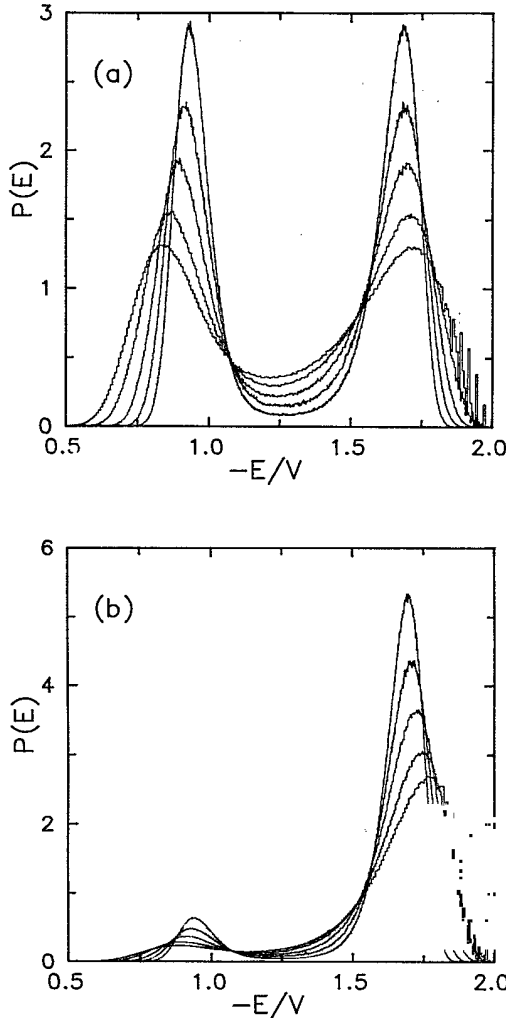


FIG. 9. Energy histograms for  $q=10$ . In (a) they are reweighted to the temperature where both peaks are of equal height. The location of the minimum between the two peaks defines the cut  $E_0$  used in the ratio-of-weights method. (b) shows the corresponding histograms at the exactly known transition point.

$$\beta_{B_{\min}} = \beta_o - \ln(q\hat{e}_o^2/\hat{e}_d^2)/V\Delta\hat{e} + \dots$$

In nontrivial models the infinite-volume transition point would have to be estimated from linear extrapolations in  $1/V$ . As can be seen in Fig. 11, in particular for weak first-order phase transitions (small  $q$ ), this can be quite misleading. Note that the next correction term  $\propto (1/V)^2$  does not improve the agreement with the data. Rather, for  $T_{C_{\max}}$  (where also this term is exactly known for Potts models) it is extremely small and even goes in the *wrong* direction. Using reasonable estimates for  $\hat{e}_o$  (which is not exactly known) the  $(1/V)^2$  correction for  $T_{B_{\min}}$  turns out to be somewhat larger, and in any case also points in the *wrong* direction. In view of the neglected exponential corrections this is not surprising at all. In fact, allowing also terms  $\propto e^{-L/L_0}$  besides the  $1/V$  corrections, and performing fits to the data, we find the interpolating dashed curves in Fig. 11. Clearly, the specific ansatz is heuristic and only justified by its numerical success. It is very difficult to get a theoretical clue on the complete form of the exponential corrections ( $L$ -dependent prefactors, linear combinations of several exponentials with slightly different  $L_0$ , etc.).

### B. Transition points from the new observables

Knowing the (optimized) probability distributions  $P_\beta(E)$ , also the positions  $\beta_{V/V}$  of the maxima of  $N(V_1, V_2, \beta)$  in Eq. (6) are readily determined. Or, equivalently, one may locate the crossing points of the energies for the two lattice sizes considered. We have chosen the volumes  $V_1$  and  $V_2$  such that their ratio  $\alpha = V_2/V_1$  is roughly constant ( $\approx 1.6$ ). The resulting curves for  $N(V_1, V_2, \beta)$  are shown in Fig. 7. Here we have fixed an unknown temperature-independent constant (corresponding to an additive constant in the free energies) by normalizing the maxima to  $q+1$ . This does certainly not affect the *position* of the maxima,  $\beta_{V/V}$ , which are plotted in Fig. 11. We see that  $\beta_{V/V}$  approach the infinite-volume transition point  $\beta_o$  quite rapidly from below, thus confirming the theoretical expectations.

Figure 8 shows a comparison of our data for  $q=8$  with the finite-size scaling prediction

$$\begin{aligned} N(V_1, V_2, \beta) &= 2\sqrt{q} \left[ \frac{\cosh[V_1\beta\Delta f/2 + (1/2)\ln q]^\alpha}{\cosh[V_2\beta\Delta f/2 + (1/2)\ln q]} \right]^{1/(\alpha-1)}, \quad (16) \end{aligned}$$

which follows by inserting (15) in definition (6). More precisely  $\beta\Delta f \equiv \beta(f_d - f_o)$  is short for its Taylor expansion around  $\beta_o$  up to second order in  $\beta - \beta_o$ , i.e.,  $\beta\Delta f$  in (16) has to be replaced by

$$\beta_o\Delta\hat{e}(\beta/\beta_o - 1) - \Delta\hat{e}(\beta/\beta_o - 1)^2/2.$$

In Fig. 8(a),  $\beta_o = \ln(1 + \sqrt{q})$  is the infinite-volume transition point, and in Fig. 8(b) we have replaced  $\beta_o$  by  $\beta_{V/V}$ , thereby taking into account already part of the exponen-



tial corrections. The corresponding plots for  $q=10$  look quite similar, while for  $q=5$  our lattices are still too small to exhibit asymptotic finite-size scaling behavior.

Our second criterion in Eq. (12) is only little more laborious to implement. First, reweighting the energy distribution using relation (9) we vary the temperature until both peaks have equal height and determine the energy  $E_0$  at the minimum between them. The numerical values of  $E_0$  can be read off from Fig. 12, and for  $q=10$  the resulting energy distributions for the various lattice sizes can be inspected in Fig. 9(a). Since the histogram data are usually quite noisy, we first smooth them by computing "moving averages"<sup>24</sup> and then fit cubic polynomials near the extrema. A good starting point for this procedure is the temperature where the specific heat is maximal (or simply the initial guess  $\beta_1$  given in Table II). Since at this temperature the two peaks have approxi-

mately equal weight, the histogram has then already roughly the desired shape (compare Fig. 1 and see Appendix B). Having fixed the cut parameter  $E_0$  and using (9) again, we finally adjust  $\beta$  until at  $\beta=\beta_W$  the ratio of weights of the ordered and disordered peak,  $R(V,\beta)$ , equals  $q$ . For  $q=10$  the energy distributions at the exactly known transition point  $\beta_0$  are shown in Fig. 9(b). In Fig. 10, the logarithm of the ratio-of-weights parameter  $R(V,\beta)$  is plotted as a function of temperature. The convergence properties of the resulting pseudotransition points  $\beta_W$  can again be inspected in Fig. 11. They turn out to approximate the infinite-volume transition point  $\beta_0$  even closer than the corresponding points  $\beta_{V/V}$ . Notice the surprisingly fast convergence even for  $q=5$ . On the larger lattices we would need much higher statistics in order to disentangle statistical errors from the small systematic deviations of the order  $|\beta_W-\beta_0|\approx 10^{-4}$ . With

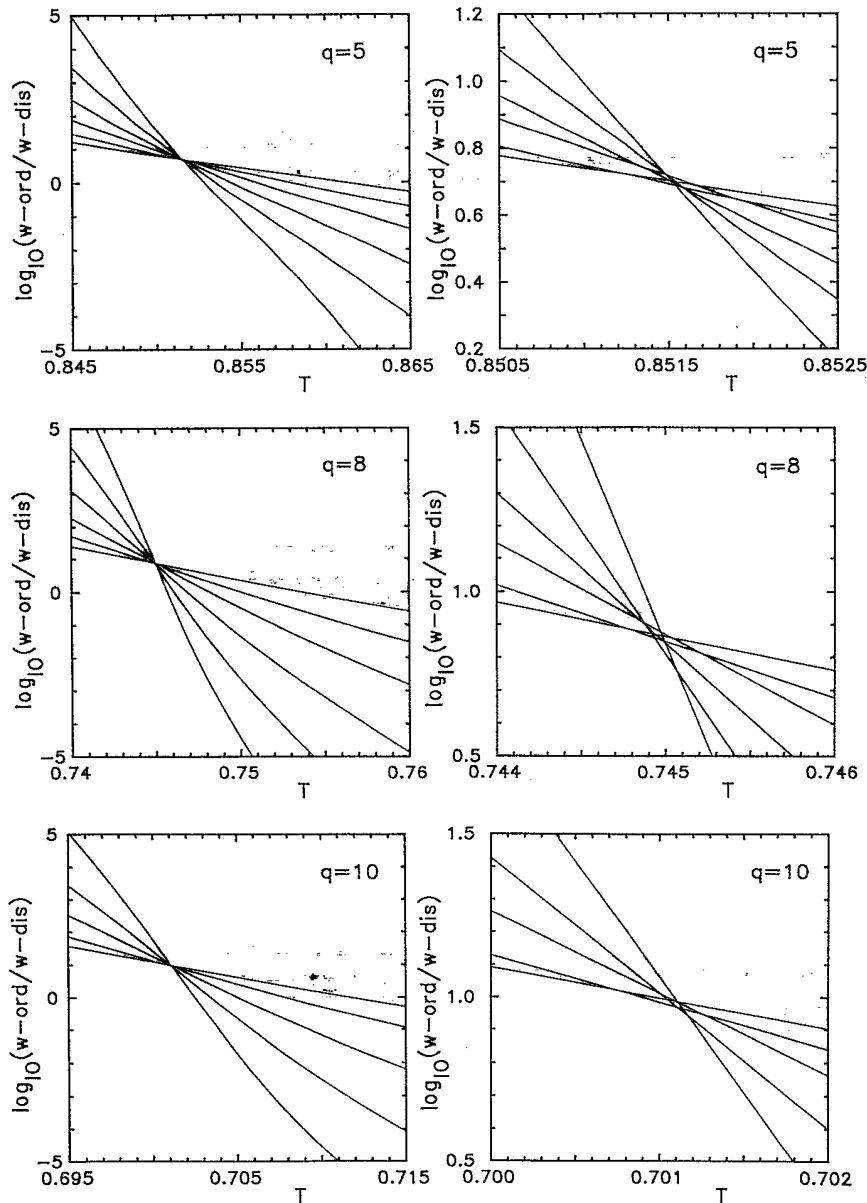


FIG. 10. The ratio-of-weights parameter for  $q=5, 8,$  and  $10$  on a logarithmic scale for various lattice sizes computed by reweighting the optimized histograms. On the right-hand panels the crossing regions are magnified by a factor of  $10$  in both the  $x$  and  $y$  directions. The statistical errors are too large to allow for a detailed analysis of the exponentially small systematic corrections.

the present data it is thus hopeless to try exponential fits to the residual deviations from  $\beta_0$ . We have checked that using other reasonable definitions for locating the cut  $E_0$  does not change the behavior of  $\beta_W$  significantly. Notice finally that we can read off from Fig. 10 also the approxi-

mate location of  $\beta_{C_{\max}}$  and  $\beta_{B_{\min}}$ . All we have to do is to draw horizontal lines at the corresponding theoretical ratio of weights, namely,  $y = \log_{10} 1 = 0$  and  $y = \log_{10}(\hat{e}_d^2/\hat{e}_o^2)$ , and to read off the  $x$  values at their crossing points with the measured  $\log_{10} R(V, \beta)$  curves.

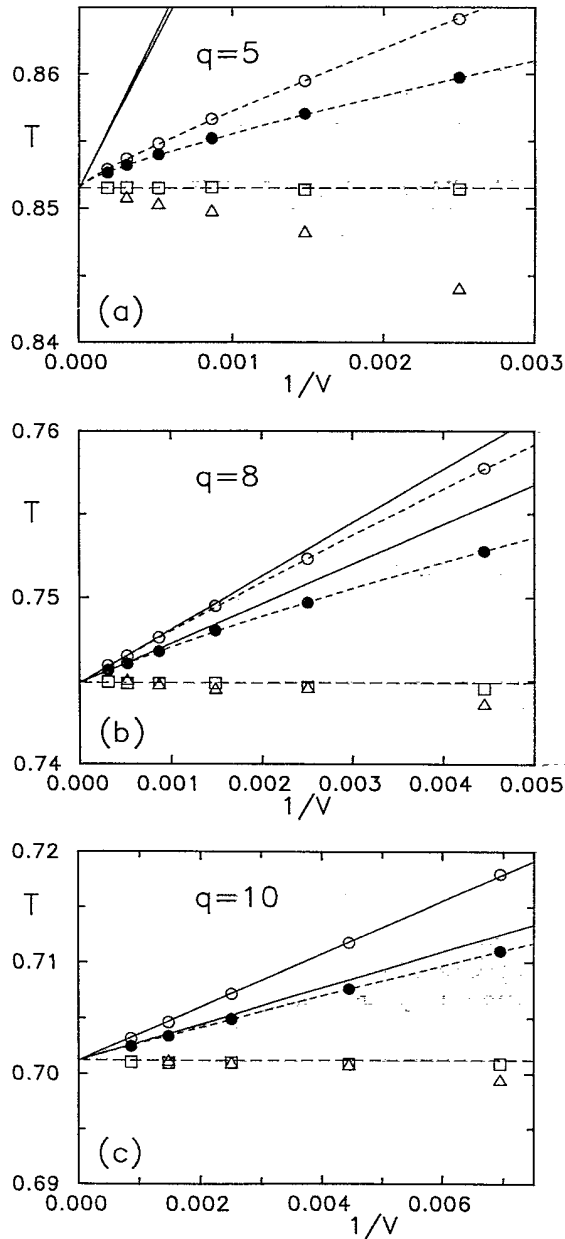


FIG. 11. Finite-volume transition points in the two-dimensional Potts model for  $q=5, 8,$  and  $10$ . Shown are the points  $\beta_{V/V}$  ( $\Delta$ ) and  $\beta_W$  ( $\square$ ), resulting from the new criteria tested in this paper and, for comparison, also the positions of the specific-heat maximum ( $\bullet$ ) and Binder-parameter minimum ( $\circ$ ). The solid straight lines are the exactly known  $1/V$  corrections corresponding to  $\bullet$  and  $\circ$ , and the dashed, almost interpolating, curves show exponential fits (including the  $1/V$  corrections) to these data. Note that the  $(1/V)^2$  corrections are almost invisible on this scale and in any case point in the "wrong" upward direction. The long-dashed horizontal lines indicate the exact transition points.

### C. Latent heat from finite-size data

Let us now turn to estimators for the latent heat on finite lattices. One method recently proposed by Lee and

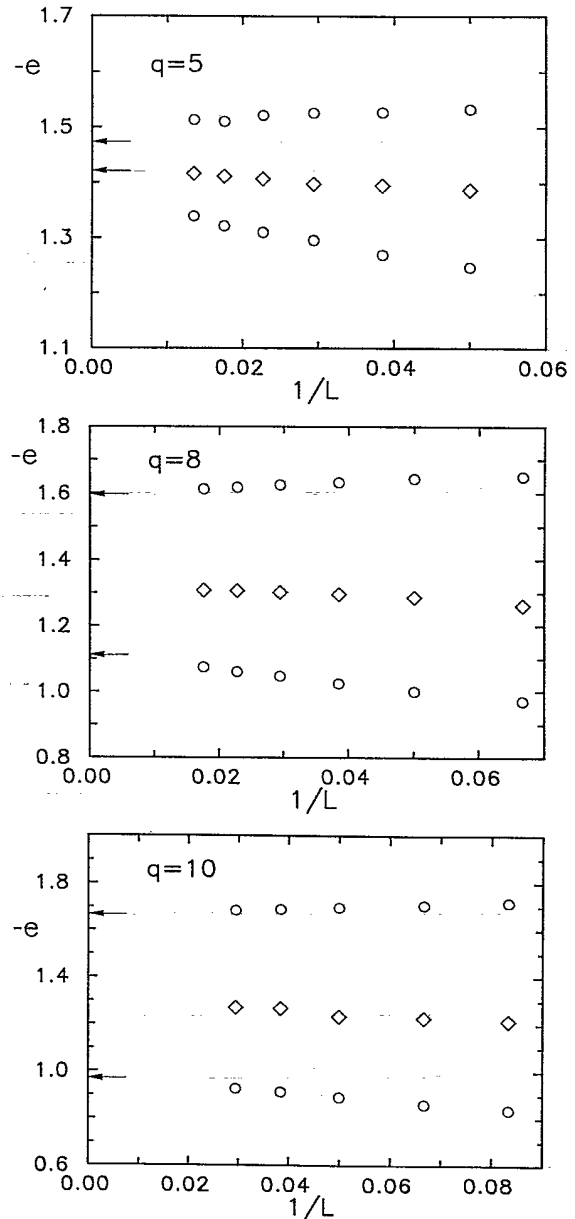


FIG. 12. Scaling of  $e_d(L)$  and  $e_o(L)$  computed from the location of the maxima for peaks of equal height. The diamonds show the corresponding minima,  $e_m$ , between the two peaks. The latter values are used for the energy cuts in the ratio-of-weights method,  $E_0 = Ve_m$ . The arrows on the  $y$  axis show the exactly known infinite volume limits  $\hat{e}_d, \hat{e}_o$ .

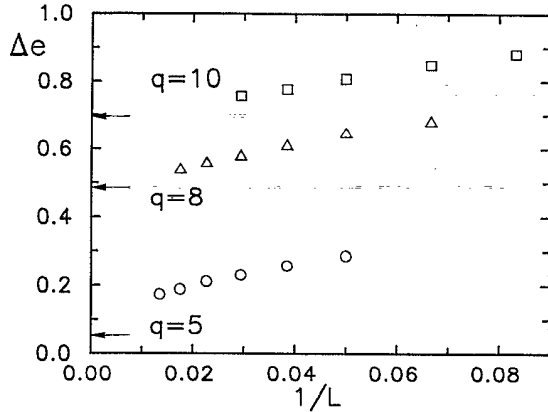


FIG. 13. Scaling of the latent heat,  $\Delta e = e_d - e_o$ , calculated from the data in Fig. 10. The arrows on the left-hand side show the exactly known infinite-volume limits.

Kosterlitz<sup>23</sup> is to reweight a given energy histogram until both peaks have equal height, as in our prescription for locating the cut parameter  $E_0$ . The locations of the peak maxima are then taken as finite-size estimates,  $e_d(L)$  and  $e_o(L)$ , for the infinite-volume limits at  $\beta_0$ ,  $\hat{e}_d$  and  $\hat{e}_o$ , and thus the latent heat  $\Delta \hat{e} = \hat{e}_d - \hat{e}_o$ . Heuristic arguments<sup>23</sup> suggest that

$$\begin{aligned} e_d(L) &= \hat{e}_d + O(1/L), \\ e_o(L) &= \hat{e}_o - O(1/L). \end{aligned} \quad (17)$$

Furthermore, one expects that at the minimum between the two peaks,  $e_m(L) \equiv E_0(V)/V$ , the microcanonical free energy,  $F(e, V) \equiv -\ln P_\beta(e, V)$ , scales as

$$\Delta F(V) \equiv F(e_m, V) - F(e_o, V) = \text{const} \times L + \dots \quad (18)$$

In Fig. 12, it is demonstrated that the predicted scaling behavior for  $e_d$  and  $e_o$  is indeed very well satisfied by our data for  $q=8$  and 10. At the extremely weak first-order transition for  $q=5$ , however, we have clearly not yet reached the asymptotic scaling region. The corresponding finite-size estimates for the latent heat are plotted in Fig. 13, and Fig. 14 shows  $\Delta F(V)/L$  as defined in Eq. (18). The extrapolated values for infinite volume are in

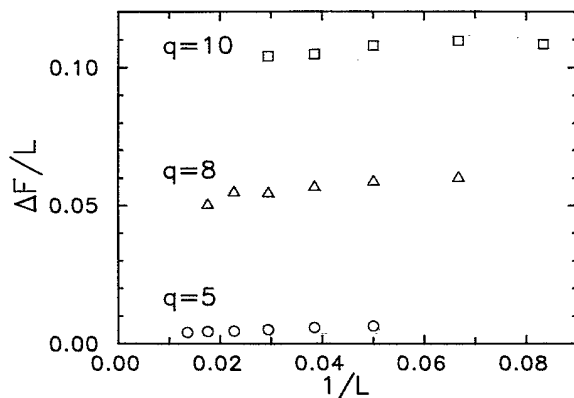


FIG. 14. Scaling of the free energy  $\Delta F(V)/L$  defined in Eq. (18). The infinite-volume limits are estimates for twice the interface tension between the disordered and ordered phases.

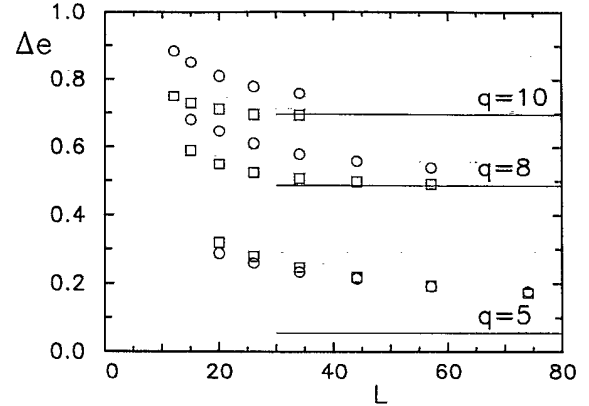


FIG. 15. The latent heat from the new ratio-of-weights method ( $\square$ ) in comparison with the standard equal-peak-height data ( $\circ$ ) already shown in Fig. 13. The horizontal lines show the exactly known infinite-volume limits.

good agreement with analytical results<sup>25</sup> and with Monte Carlo simulations using the recently proposed<sup>26</sup> multi-canonical ensemble which yield  $\text{const} = 0.09781 \pm 0.00075$  for  $q=10$ ,<sup>27</sup> and  $\text{const} = 0.0241 \pm 0.0010$  for  $q=7$ .<sup>28</sup>

The ratio-of-weights method to locate the transition point leads naturally to another definition of the latent heat on finite lattices which also should have only exponentially small corrections with respect to the infinite-volume limit. Since

$$\ln(w_o/w_d) = -\beta V(f_o - f_d), \quad (19)$$

the slopes of  $R(V, \beta)$  in Fig. 10 near the crossing point may be used to define

$$\begin{aligned} \Delta e(L) &= e_d(L) - e_o(L) = \frac{d}{d\beta} \ln(W_o/W_d)/V \\ &= -\frac{1}{T^2} \frac{d}{dT} \ln(W_o/W_d)/V. \end{aligned} \quad (20)$$

The resulting estimates  $\Delta e(L)$  are plotted in Fig. 15 and compared with the previous definition. We see that for  $q=8$  and 10 the asymptotic limit is indeed reached much faster with the new definition, and that the approach of the infinite-volume limit looks roughly exponential. For  $q=5$ , on the other hand, both methods yield comparable estimates which are still far away from the limiting value.

## V. CONCLUSION

In summary, we have successfully tested two simple criteria for locating first-order phase-transition points in Monte Carlo simulations on finite periodic lattices which have only exponentially small corrections with respect to the infinite-volume limit. In particular, the ratio-of-weights methods works surprisingly well also for very weak first-order phase transitions such as in the two-dimensional  $q=5$  Potts model. Since a possible reason for this could be a fortuitous cancellation of exponential corrections, it would be interesting to investigate this issue for other models with weak first-order transitions.

Based on the ratio-of-weights approach we finally propose a method to determine the latent heat from finite-size data. The numerical tests of this method show that for moderate and strong first-order phase-transitions the infinite-volume limit of the latent heat is approached much faster than with previously used finite lattice definitions.

#### ACKNOWLEDGMENTS

The methods tested in this paper have been developed in collaboration with Christian Borgs. It is a pleasure to thank him for many stimulating discussions during the whole project. Further, I would like to thank Bernd Berg and Alain Billoire for helpful discussions. Work supported in part by Deutsche Forschungsgemeinschaft under Grant No. K1256.

#### APPENDIX A: SUMMARY OF EXACT RESULTS

The two-dimensional Potts model with energy  $E = -\sum_{\langle x, x' \rangle} \delta_{s(x)s(x')}$  exhibits for  $q \geq 5$  a first-order phase transition at the inverse temperature<sup>18</sup>

$$\beta_0 = \ln(1 + \sqrt{q}), \quad (\text{A1})$$

with average internal energy

$$-\frac{\hat{e}_o + \hat{e}_d}{2} = 1 + 1/\sqrt{q}, \quad (\text{A2})$$

and latent heat

$$\begin{aligned} \Delta\hat{e} &\equiv \hat{e}_d - \hat{e}_o \\ &= 2(1 + 1/\sqrt{q}) \tanh(\Theta/2) \prod_{n=1}^{\infty} \tanh^2(n\Theta), \end{aligned} \quad (\text{A3})$$

where

$$2 \cosh \Theta = \sqrt{q}, \quad \Theta = \ln(\sqrt{q/4} + \sqrt{q/4 - 1}). \quad (\text{A4})$$

The corresponding entropy jump is

$$\Delta\hat{s} = \beta_0 \Delta\hat{e} > 0. \quad (\text{A5})$$

For the specific heats only the difference between the disordered and ordered phase is known exactly,

$$\Delta\hat{c} = \hat{c}_d - \hat{c}_o = \beta_0 \Delta\hat{s} / \sqrt{q}. \quad (\text{A6})$$

The numerical values for  $q = 5, 8,$  and  $10$  are compiled in Table I.

#### APPENDIX B: FINITE-SIZE SCALING

In this appendix  $T_0$  denotes the infinite-volume transition temperature,  $T_{C_{\max}}$  and  $T_{B_{\min}}$  refer to the location of the specific-heat maximum and Binder-parameter minimum, respectively, and  $T_p$  is the temperature where both peaks have equal weight. Furthermore, we shall use the latent heat, transition entropy, and specific-heat jump,

$$\Delta\hat{e} \equiv \hat{e}_d - \hat{e}_o > 0, \quad (\text{B1})$$

$$\Delta\hat{s} \equiv (\hat{e}_d - \hat{e}_o) / T_0 > 0, \quad (\text{B2})$$

$$\Delta\hat{c} \equiv \hat{c}_d - \hat{c}_o \stackrel{\text{Potts}}{=} \Delta\hat{s} / T_0 \sqrt{q} > 0, \quad (\text{B3})$$

where the caret denotes quantities evaluated at  $T_0$ , and the subscripts refer to the disordered or ordered phases. The second equality in (B3) is only valid for the two-dimensional Potts model (see Appendix A). In what follows the leading terms of the asymptotic expansions in  $1/V$  are given for the specific heat and the Binder parameters. For  $q = 5, 8,$  and  $10$  the numerical values of the exactly known expansion coefficients are compiled in Table III.

##### 1. Specific heat [ $C = \beta^2 V (\langle e^2 \rangle - \langle e \rangle^2)$ ]

At  $T_0$ ,

$$\begin{aligned} C(T_0) &= V \frac{4q}{(1+q)^2} \left[ \frac{\Delta\hat{s}}{2} \right]^2 + \frac{q-1}{q+1} \frac{\Delta\hat{c}}{2} + \frac{\hat{c}_d + \hat{c}_o}{2} \\ &= V \frac{4q}{(1+q)^2} \left[ \frac{\Delta\hat{s}}{2} \right]^2 + \frac{\Delta\hat{c}}{1+q} + \hat{c}_o. \end{aligned} \quad (\text{B4})$$

At the equal peak weight,

$$\begin{aligned} T_p &= T_0 + \frac{T_0}{V \Delta\hat{s}} \ln q + \frac{T_0}{(V \Delta\hat{s})^2} \left[ 1 - \frac{\Delta\hat{c}}{2 \Delta\hat{s}} \right] (\ln q)^2 \\ &\quad + O(1/V^3), \end{aligned} \quad (\text{B5})$$

$$\begin{aligned} C_p &= V \left[ \frac{\Delta\hat{s}}{2} \right]^2 + \frac{c_d + c_o}{2}, \\ &= V \left[ \frac{\Delta\hat{s}}{2} \right]^2 + \frac{(\Delta\hat{c} - \Delta\hat{s}) \ln q}{2} + \frac{\hat{c}_d + \hat{c}_o}{2} + O(1/V). \end{aligned} \quad (\text{B6})$$

At the specific-heat maximum,

$$T_{C_{\max}} = T_0 + \frac{T_0}{V \Delta\hat{s}} \ln q + \frac{T_0}{(V \Delta\hat{s})^2} \left[ 6 \frac{\Delta\hat{c}}{\Delta\hat{s}} - 4 + \left[ 1 - \frac{\Delta\hat{c}}{2 \Delta\hat{s}} \right] (\ln q)^2 \right] + O(1/V^3), \quad (\text{B7})$$

$$\begin{aligned} C_{\max} &= V \left[ \frac{\Delta\hat{s}}{2} \right]^2 + \frac{(\Delta\hat{c} - \Delta\hat{s}) \ln q}{2} + \frac{\hat{c}_d + \hat{c}_o}{2} + O(1/V) \\ &= V \left[ \frac{\Delta\hat{s}}{2} \right]^2 + \frac{\Delta\hat{c} + (\Delta\hat{c} - \Delta\hat{s}) \ln q}{2} + \hat{c}_o + O(1/V). \end{aligned} \quad (\text{B8})$$

Notice that

$$T_{C_{\max}} = T_p + O(1/V^2) \stackrel{\text{Potts}}{<} T_p$$

and  $C_{\max} = C_p + O(1/V)$  ( $> C_p$  by definition).

## 2. Binder parameter ( $B = 1 - \langle e^4 \rangle / 3 \langle e^2 \rangle^2$ )

At  $T_0$ ,

$$B(T_0) = 1 - \frac{1+q}{3} \frac{q\hat{e}_o^4 + \hat{e}_d^4}{(q\hat{e}_o^2 + \hat{e}_d^2)^2} - \frac{T_0^2}{3V} \frac{1+q}{(q\hat{e}_o^2 + \hat{e}_d^2)^2} \left[ 6(q\hat{e}_o^2\hat{c}_o + \hat{e}_d^2\hat{c}_d) - 2 \frac{q\hat{e}_o^4 + \hat{e}_d^4}{q\hat{e}_o^2 + \hat{e}_d^2} (q\hat{c}_o + \hat{c}_d) \right]. \quad (\text{B9})$$

At the specific-heat maximum,

$$B(T_{C_{\max}}) = 1 - \frac{2}{3} \frac{\hat{e}_d^4 + \hat{e}_o^4}{(\hat{e}_d^2 + \hat{e}_o^2)^2} + O(1/V) = \frac{2}{3} - \frac{1}{3} \frac{(\hat{e}_d^2 - \hat{e}_o^2)^2}{(\hat{e}_d^2 + \hat{e}_o^2)^2} + O(1/V). \quad (\text{B10})$$

At the Binder-parameter minimum,

$$T_{B_{\min}} = T_0 + \frac{T_0}{V\Delta\hat{s}} \ln(q\hat{e}_o^2/\hat{e}_d^2) + \frac{T_0}{(V\Delta\hat{s})^2} \left\{ \ln(q\hat{e}_o^2/\hat{e}_d^2) \left[ \left[ 1 - \frac{\Delta\hat{c}}{2\Delta\hat{s}} \right] \ln(q\hat{e}_o^2/\hat{e}_d^2) + 2T_0 \left[ \frac{\hat{c}_o}{\hat{e}_o} - \frac{\hat{c}_d}{\hat{e}_d} \right] \right] \right. \\ \left. + \frac{\hat{c}_d\hat{e}_o^2 - \hat{c}_o\hat{e}_d^2}{\Delta\hat{s}(\hat{e}_o + \hat{e}_d)^2} \left[ 10 - \frac{\hat{e}_o^2}{\hat{e}_d^2} - \frac{\hat{e}_d^2}{\hat{e}_o^2} \right] - 4 \frac{\hat{e}_o^2 + \hat{e}_d^2}{\Delta\hat{s}(\hat{e}_o + \hat{e}_d)} \left[ \frac{\hat{c}_o}{\hat{e}_o} - \frac{\hat{c}_d}{\hat{e}_d} \right] \right\} + O(1/V^3), \quad (\text{B11})$$

$$B_{\min} = 1 - \frac{1}{12} \left[ \frac{\hat{e}_o}{\hat{e}_d} + \frac{\hat{e}_d}{\hat{e}_o} \right]^2 - \frac{T_0^2}{12V} \frac{\hat{e}_o^2 + \hat{e}_d^2}{\hat{e}_o^2\hat{e}_d^2} \left[ -2(\hat{e}_o + \hat{e}_d) \left[ \frac{\hat{c}_o}{\hat{e}_o} - \frac{\hat{c}_d}{\hat{e}_d} \right] \ln(q\hat{e}_o^2/\hat{e}_d^2) + 6(\hat{c}_o + \hat{c}_d) - (\hat{e}_o^2 + \hat{e}_d^2) \left[ \frac{\hat{c}_o}{\hat{e}_o^2} + \frac{\hat{c}_d}{\hat{e}_d^2} \right] \right] \\ + O(1/V^2). \quad (\text{B12})$$

The leading term can be rewritten as

$$B_{\min} = \frac{2}{3} - \frac{1}{12} \left[ \frac{\hat{e}_o}{\hat{e}_d} - \frac{\hat{e}_d}{\hat{e}_o} \right]^2 + O(1/V), \quad (\text{B13})$$

showing that  $\lim_{V \rightarrow \infty} B_{\min} < \frac{2}{3}$ . Notice that the  $O(1/V^2)$  term for  $T_{B_{\min}}$  and the  $O(1/V)$  term for  $B_{\min}$  are *not* exactly known for Potts models since they involve both  $\hat{c}_o$  and  $\hat{c}_d$  and not only the combination  $\Delta\hat{c} = \hat{c}_d - \hat{c}_o$  (as is the case for the corresponding expansions of the specific heat).

## 3. Connected Binder parameter

$$[B^c = 1 - \langle (e - \langle e \rangle)^4 \rangle / 3 \langle (e - \langle e \rangle)^2 \rangle^2]$$

At  $T_0$ ,

$$B^c = -\frac{1}{3} \left[ q + \frac{1}{q} - 4 \right] + O(1/V). \quad (\text{B14})$$

At the connected Binder-parameter maximum,

$$T_{B_{\max}^c} = T_0 + \frac{T_0}{V\Delta\hat{s}} \ln q \\ + \frac{T_0}{(V\Delta\hat{s})^2} \left[ 4 \frac{\Delta\hat{c}}{\Delta\hat{s}} + \left[ 1 - \frac{1}{2} \frac{\Delta\hat{c}}{\Delta\hat{s}} \right] (\ln q)^2 \right] \\ + O(1/V^3), \quad (\text{B15})$$

$$B_{\max}^c = \frac{2}{3} - \frac{1}{V\Delta\hat{s}} \frac{8(\hat{c}_o + \hat{c}_d)}{3\Delta\hat{s}} + O(1/V^2). \quad (\text{B16})$$

<sup>1</sup>M. E. Fisher and A. N. Berker, Phys. Rev. B **26**, 2507 (1982).

<sup>2</sup>V. Privman and M. E. Fisher, J. Stat. Phys. **33**, 385 (1983).

<sup>3</sup>K. Binder and D. P. Landau, Phys. Rev. B **30**, 1477 (1984).

<sup>4</sup>M. S. S. Challa, D. P. Landau, and K. Binder, Phys. Rev. B **34**, 1841 (1986).

<sup>5</sup>V. Privman and J. Rudnik, J. Stat. Phys. **60**, 551 (1990).

<sup>6</sup>For a recent review, see V. Privman, in *Finite-Size Scaling and Numerical Simulations of Statistical Physics*, edited by V.

Privman (World Scientific, Singapore, 1990).

<sup>7</sup>K. Binder, Z. Phys. B **43**, 119 (1981).

<sup>8</sup>For the scaling behavior in long cylinders, see, e.g., Ref. 2 and C. Borgs and J. Z. Imbrie, Commun. Math. Phys. **145**, 235 (1992).

<sup>9</sup>A special case with  $\alpha=2$  happens if the number of stable phases on both sides of the transition are equal, see Refs. 10 and 11.

- <sup>10</sup>C. Borgs and R. Kotecký, *J. Stat. Phys.* **61**, 79 (1990); *Phys. Rev. Lett.* **68**, 1734 (1992).
- <sup>11</sup>C. Borgs, R. Kotecký, and S. Miracle-Solé, *J. Stat. Phys.* **62**, 529 (1991).
- <sup>12</sup>C. Borgs and W. Janke, *Phys. Rev. Lett.* **68**, 1738 (1992).
- <sup>13</sup>For technical details, see Refs. 10 and 11.
- <sup>14</sup>If the energy distribution is continuous, the sum over  $E$  becomes an integral and  $N(E)$  is replaced by the spectral density  $\rho(E)=dN(E)/dE$ . To simplify the notation we have suppressed the lattice size dependence of  $N(E)$  and of the range of summation.
- <sup>15</sup>A. M. Ferrenberg and R. H. Swendsen, *Phys. Rev. Lett.* **61**, 2635 (1988); **63**, 1658(E) (1989).
- <sup>16</sup>A. M. Ferrenberg and R. H. Swendsen, *Phys. Rev. Lett.* **63**, 1195 (1989).
- <sup>17</sup>For a general review of the Potts model, see, e.g., F. Y. Wu, *Rev. Mod. Phys.* **54**, 235 (1982); **55**, 315E (1983).
- <sup>18</sup>R. J. Baxter, *J. Phys. C* **6**, L445 (1973).
- <sup>19</sup>R. H. Swendsen and J. S. Wang, *Phys. Rev. Lett.* **58**, 86 (1987).
- <sup>20</sup>U. Wolff, *Phys. Rev. Lett.* **62**, 361 (1989).
- <sup>21</sup>W. Janke (unpublished).
- <sup>22</sup>It should be stressed once again that our choice of  $\beta_0$  as one simulation point was convenient but by no means essential for testing the usefulness of the observables defined in Sec. II, which are just designed for a precise determination of  $\beta_0$ .
- <sup>23</sup>J. Lee and J. M. Kosterlitz, *Phys. Rev. Lett.* **65**, 137 (1990); *Phys. Rev. B* **43**, 3265 (1991).
- <sup>24</sup>S. Brandt, *Datenanalyse* (Bibliographisches Institut, Mannheim, 1981).
- <sup>25</sup>C. Borgs and W. Janke, *J. Phys. I (Paris)* **2**, 2011 (1992).
- <sup>26</sup>B. A. Berg and T. Neuhaus, *Phys. Lett. B* **267**, 249 (1991).
- <sup>27</sup>B. A. Berg and T. Neuhaus, *Phys. Rev. Lett.* **68**, 9 (1992).
- <sup>28</sup>W. Janke, B. A. Berg, and M. Katoot, *Nucl. Phys. B* **382**, 649 (1992). W. Janke, in *Dynamics of First Order Phase Transitions*, Proceedings of the HLRZ Workshop, Forschungszentrum Jülich, 1992, edited by H. J. Herrmann, W. Janke, and F. Karsch (World Scientific, Singapore, 1992), p. 365, reprinted in *Int. J. Mod. Phys. C* **3**, 1137 (1992).